Surface & Coatings Technology 204 (2009) 85–90

Contents lists available at ScienceDirect

Surface & Coatings Technology

journal homepage: www.elsevier.com/locate/surfcoat

Characterization and frictional behavior of nanostructured Ni–W–MoS_2 composite coatings

M.F. Cardinal [a], P.A. Castro [a], J. Baxi [c], H. Liang [c], F.J. Williams [a,b,*]

[a] Surface Chemistry and Coatings Department, TENARIS Research and Development Centre, Simini 250, Campana 2804, Argentina
[b] Departamento de Química Inorgánica, Analítica y Química Física, Facultad de Ciencias Exactas y Naturales, Universidad de Buenos Aires, Ciudad Universitaria, C1428EGA, Buenos Aires, Argentina
[c] Department of Mechanical Engineering, Texas A&M University, College Station, TX 77843-3123, USA

ARTICLE INFO

Article history:
Received 8 October 2008
Accepted in revised form 24 June 2009
Available online 3 July 2009

Keywords:
Nanostructured
Coating
Electrodeposition
Solid lubricant
Ni–W
MoS2

ABSTRACT

Ni–W–MoS_2 composite coatings were obtained by pulse plating from a Ni–W electrolyte containing suspended MoS_2 particles. The coating composition, morphology, crystalline structure, microhardness and frictional behavior were studied as a function of MoS_2 concentration. The results obtained in this study indicate that co-deposited lubricant particles strongly influenced the composite Ni–W coating properties. It was found that increasing co-deposited MoS_2 diminished tungsten content in the coating and consequently increased the average grain size. Ni–W nanostructured coatings with high MoS_2 content have a porous sponge-like structure, high surface roughness and irregular frictional behavior. However, the friction coefficient of Ni–W coatings is reduced to half its value with low MoS_2 content.

1. Introduction

Innovative coatings with enhanced mechanical properties are constantly required for several industrial applications. It is well known that composite electroplating is an inexpensive method for achieving wear resistance, corrosion protection, oxidation resistance and self-lubrication. Many Ni composites with co-deposited insoluble particles such as lubricants (h-BN, MoS_2, SiN, PTFE, and graphite), carbides (SiC and WC), hard oxides (Al_2O_3, TiO_2, SiO_2, CeO_2, ZrO_2) and carbon nanotubes have been studied. For example, Ni–BN composite coatings with improved hardness and wear resistance were obtained by Ramesh Bapu [1] and Natarajan et al. [2]. The electrolytic co-deposition of MoS_2 with nickel was studied by Chang et al. [3], whereas co-deposition of PTFE was studied by Berçot et al. [4] and Szeptycka et al. [5]. Basu et al. [6] observed that the addition of WC into Ni coatings increased its hardness and decreased the friction coefficient of the final deposit. Micro- and nano-sized SiC particles were co-deposited with nickel from different plating baths and the amount of SiC in the coating determined the microhardness, wear and corrosion resistance of the composite coatings [7–9].

Ni–W nanostructured alloys are known to exhibit superior mechanical and chemical properties than Ni coatings. Therefore, there has been a considerable amount of work devoted to understanding how the deposition parameters affect the hardness, wear, heat and corrosion resistance of Ni–W coatings [10–15]. Despite all this effort, there have been only a few studies regarding the electrodeposition of Ni–W composite coatings with co-deposited insoluble particles. Recently, Yao et al. [16,17] electrodeposited Ni–W–SiC composite coatings and investigated the influence of plating conditions on its composition and properties; increasing the SiC concentration in the plating bath resulted in an increased amount of co-deposited nanoparticles and consequently in an increased microhardness. Furthermore, Ni–W–SiC nanocomposite coatings showed better wear and corrosion resistance properties than Ni–W coatings.

MoS_2 is a diamagnetic semiconducting material with applications as a solid lubricant for tribological applications in high temperature and vacuum environments where the use of traditional liquid lubricants becomes ineffective or cannot be tolerated [18]. MoS_2 has a layered lattice structure wherein molybdenum atoms are sandwiched between layers of sulfur atoms (S–Mo–S) and are held together strongly by covalent bonding. The interaction between (S–Mo–S) layers is only by weak van der Waals forces being loosely bound to each other. Such a layered crystallographic arrangement allows the MoS_2 layers to easily shear between basal planes and is responsible for its excellent lubricity. In the present work we co-deposited a MoS_2 into a Ni–W alloy in order to generate a coating with low friction coefficient. Ni–W–MoS_2 composite coatings with varying MoS_2 content were prepared by means of reverse pulse plating on carbon steel samples. We studied the incorporation of MoS_2 particles into a Ni–W matrix as a function of the MoS_2 bath concentration. The morphology and crystalline structure of the electrodeposited coatings

* Corresponding author. Surface Chemistry and Coatings Department, TENARIS Research and Development Centre, Simini 250, Campana 2804, Argentina. Tel.: +54 3489 435087; fax: +54 3489 427928.
E-mail address: fwilliams@qi.fcen.uba.ar (F.J. Williams).

0257-8972/$ – see front matter © 2009 Elsevier B.V. All rights reserved.
doi:10.1016/j.surfcoat.2009.06.037

Table 1
Plating conditions.

Forward current (I_{fwd})	0.2 A/cm^2
Forward time (T_{fwd})	20 ms
Reverse current (I_{rev})	0.05 A/cm^2
Reverse time (T_{rev})	3 ms
Bath	$NiSO_4 \cdot 6H_20$ 16 g/L
	$Na_2WO_4 \cdot 2H_20$ 46 g/L
	NH_4Cl 27 g/L
	$Na_3C_6H_5O_7 \cdot 2H_20$ 147 g/L
	SDS 0.1 g/L
	MoS_2 (3 μm average particle size) from 0 to 2 g/L
Bath temperature	75 °C
pH bath	9–9.5 (addition of NH_4OH when necessary)
Plating duration	1 h
Counter electrode	Pure platinum mesh

were studied by means of X-ray diffraction, scanning electron microscopy and microhardness measurements and the frictional behavior of the composite coatings was evaluated with a pin-on-disc tribometer.

2. Experimental

Nanocrystalline Ni–W composites were prepared by reverse pulse plating. The plating bath compositions and conditions used in this study are shown in Table 1, all chemicals employed were analytical reagent-grade. Electrodepositions were carried out on carbon steel plates cut from standard "Q-panels" (SAE 1008/1010) with the edges and the back covered with an acrylic resin. Prior to each deposition, cathodes were mechanically polished, anodically etched in NaOH solution, rinsed in deionized water, pickled in a H_2SO_4 solution and rinsed again in deionized water. A fresh plating bath was used every time a new electrodeposition was carried out.

Molykote® Z Powder (Dow Corning Corporation) MoS_2 solid lubricant (average particle size of 3 μm, 98% purity and theoretical density of 4.8 g/cm^3), which is stable in the alkaline electrodeposition conditions employed in this work, was used. Sodium dodecyl sulfate (SDS) was added as a surfactant to improve the suspension and dispersion of the MoS_2 particles and prevent agglomeration of MoS_2 particles in solution.

The pulse current waveform was applied with an Autolab PG30 potentiostat. Temperature was controlled during the electrodepositions by flowing water through a water jacketed electrochemical glass cell from a Julabo® thermostatic recirculating bath. A platinum mesh anode was positioned at 5 cm distance parallel to the cathode surface. Magnetic stirring using a PTFE coated stirring bar was provided.

The coating surface morphology and chemical composition was analyzed using a Philips XL-30 scanning electron microscopy (SEM) with an energy dispersive spectroscopy (EDS) detector. X-ray diffraction (XRD) measurements were carried out on a Philips analytical X'Pert-MPD System X-Ray diffractometer using Cu Kα radiation. The average grain size was quantified by applying the integral breadth method to the (111) family of peaks [19]. Microhardness measurements were carried out on a Leco Microindenter model LM 247AT with a Vickers indenter. Microhardness measurements were performed applying a load of 50 g for 15 s. Given the large roughness of the composite coating measurements were carried out on the coating cross section. Here we should note that some Ni–W–MoS_2 composite coatings are porous with a very irregular sponge-like morphology (see Fig. 3 below), therefore microhardness measurements have a considerable error and should be taken as gross estimations in these cases.

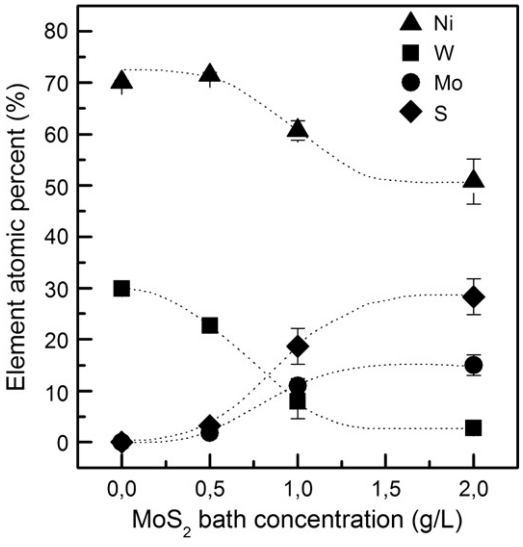

Fig. 1. SEM-EDS chemical composition of the coatings versus MoS_2 bath concentration.

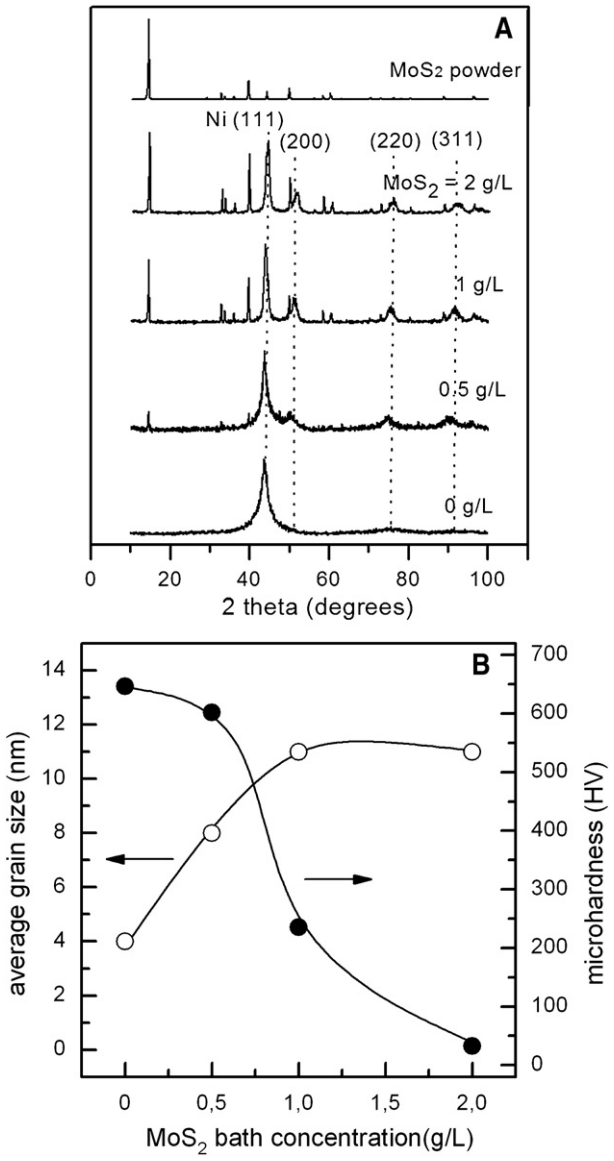

Fig. 2. (A) X-ray diffractograms for Ni–W–MoS_2 composites and MoS_2 solid lubricant as a function of MoS_2 bath concentration. (B) Dependence of average grain size (left axis) and microhardness (right axis) on MoS_2 bath concentration.

A pin-on-disc tribometer ("Standard Tribometer", CSM Instruments) was utilized to determine the friction coefficient of the coatings. Friction measurements were carried out at room temperature in dry conditions with linear mode acquisition and 2 mm half amplitude, a maximum linear speed of 1.03 cm/s, a normal load of 6 N, 2955 cycles and an acquisition rate of 10 Hz. The static partner was an uncoated stainless steel ball of 6 mm diameter cleaned with acetone. Friction coefficient measurements were carried out over Ni–W–MoS_2 coatings deposited over 1 cm × 1 cm steel samples as described above.

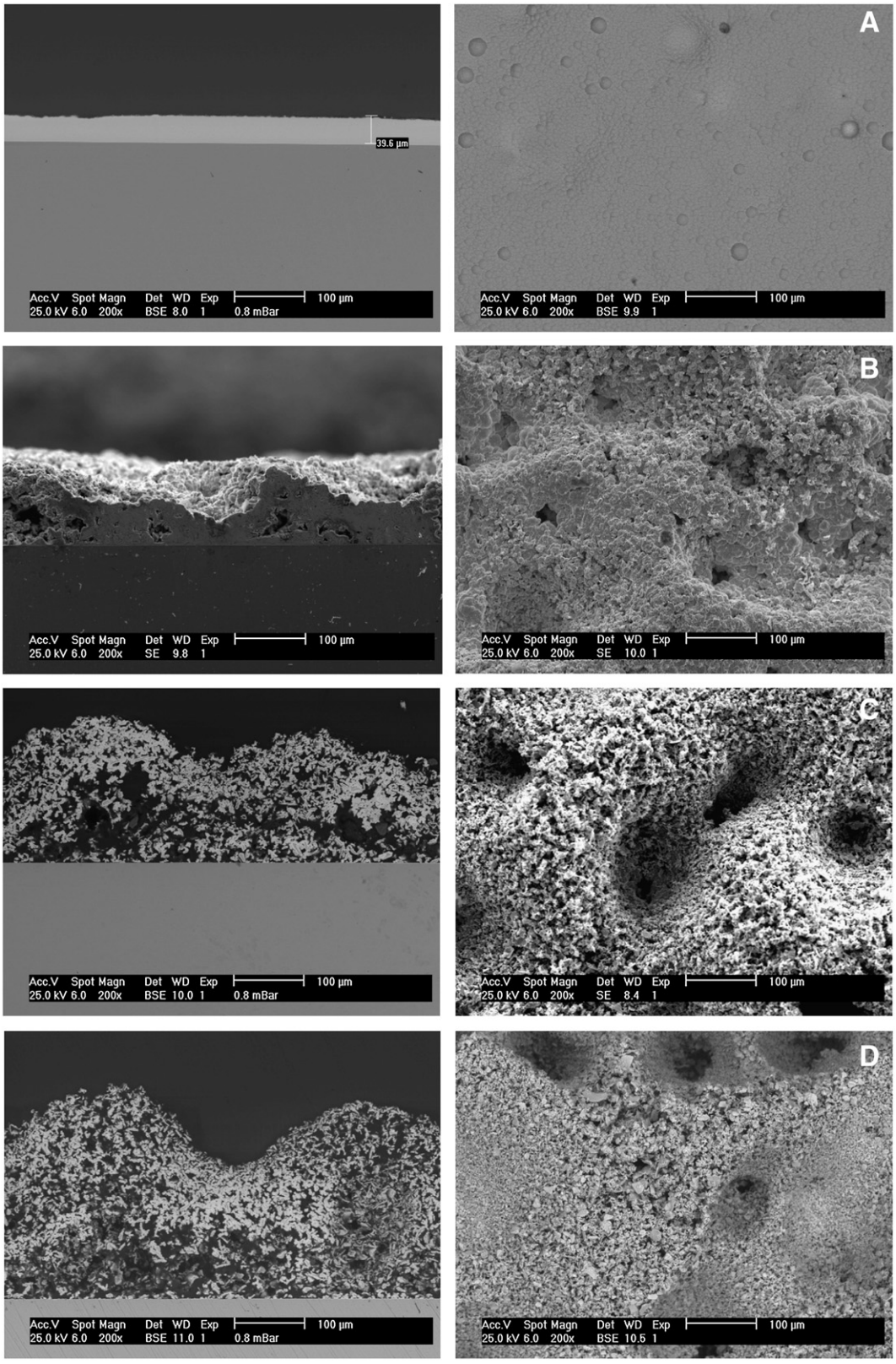

Fig. 3. Top and cross section (left) and top (right) SEM images of Ni–W electrodeposits as a function of increasing MoS_2 bath concentration. (A) 0 g/L, (B) 0.5 g/L, (C) 1 g/L and (D) 2 g/L.

3. Results and discussion

Pulse plating parameters are used to control the coating chemical composition, its grain size and hardness. For example, as the polarity ratio ($Q = I_{rev} \cdot T_{rev} / I_{fwd} \cdot T_{fwd}$) increases (current density decreases), the atomic percentage of W incorporated into the coating decreases and consequently the average grain size increases and microhardness decreases [11,12]. On the contrary, when the W content increases the average grain size diminishes and hardness increases. In the present work, we prepared Ni–W–MoS_2 composite coatings using a Ni–W electrolyte containing varying concentrations (0–2 g/L) of suspended 3 μm mean size MoS_2 particles and a polarity ratio $Q = 0.0375$. We chose this value of Q as it results in Ni–W coatings with maximum hardness when no MoS_2 is co-deposited. The chemical composition of the as-deposited composites was obtained by SEM-EDS analysis. Ni Lα, W Mα S Kα and Mo Lα lines were carefully selected to quantify the atomic percent of each element in the coating. Atomic percentages were calculated as the average value of at least 5 SEM-EDS measurements. Fig. 1 shows the Ni, W, S and Mo atomic concentrations in the composite coating as a function of the MoS_2 plating bath concentration. Increasing sulfur and Mo atomic percent with the increasing MoS_2 bath concentration indicates increasing co-deposition of molybdenum disulfide into the coating as expected. It should be noted that the relation S:Mo ~1.9 in close agreement with the stoichiometry of MoS_2. Fig. 1 also shows that as the MoS_2 bath concentration increases the atomic percent of Ni and W decreases mirroring the increased MoS_2 content, at maximum MoS_2 bath concentration there is no detectable W in the coating. Then, increasing the MoS_2 concentration in the coating has a similar effect in the coating composition as decreasing the current density (increasing the polarity ratio Q) as shown in the literature [12]. This observation will have a direct impact on the observed increased average grain sizes and might be explained as follows. As MoS_2 semiconducting particles are deposited over the electrode surface, they behave as microcathodes increasing the effective area and therefore causing a local decrease in current density which in turn results in a decrease in W content and increase in average grain size (see below).

The crystalline structure of Ni–W alloys is strongly influenced by the incorporation of the solid lubricant. Fig. 2A shows the X-ray diffraction patterns of MoS_2 powder and Ni–W–MoS_2 composite coatings for different MoS_2 bath concentrations. Clearly, as the MoS_2 bath concentration increases the diffraction peaks associated with Ni (111) sharpened indicating a decrease in the average grain sizes (see Fig. 2B). In addition, as the MoS_2 bath concentration increases the peaks associated with MoS_2 become more evident which is indicative of the increased incorporation of the solid lubricant into the coating in agreement with the results discussed in Fig. 1A. Fig. 2B shows the average grain size (left axis) and microhardness (right axis) of the Ni–W–MoS_2 composite nanostructured coating as a function of increasing MoS_2 bath concentration. Average grain sizes were calculated from the width of the Ni (111) peaks observed in the X-ray diffractograms [19]. It is well documented that Ni–W coatings electrodeposited under the conditions used in our investigation have average grain sizes in the nanometer range below 10 nm [11,20–22], which are in line with the estimated average grain sizes shown in Fig. 2B [15]. Clearly, the average grain size increases with the amount of MoS_2 co-deposited in the Ni–W alloy, which takes place with the simultaneous decrease in W content [15] and is explained in terms of a MoS_2 induced reduction in current density (see above). Fig. 2B shows that the microhardness decreased gradually from ~650 HV to ~33 HV as the MoS_2 bath concentration was increased from 0 to 2 g/L. As we shall see below this drastic decrease in microhardness is related with the porous sponge-like structure of the resulting coatings at high MoS_2 concentration. It should be noted that microhardness measurements corresponding to large MoS_2 concentration (>1 g/L) have a considerable error due to the structure of the coatings, however they correctly indicate the drastic decrease in microhardness.

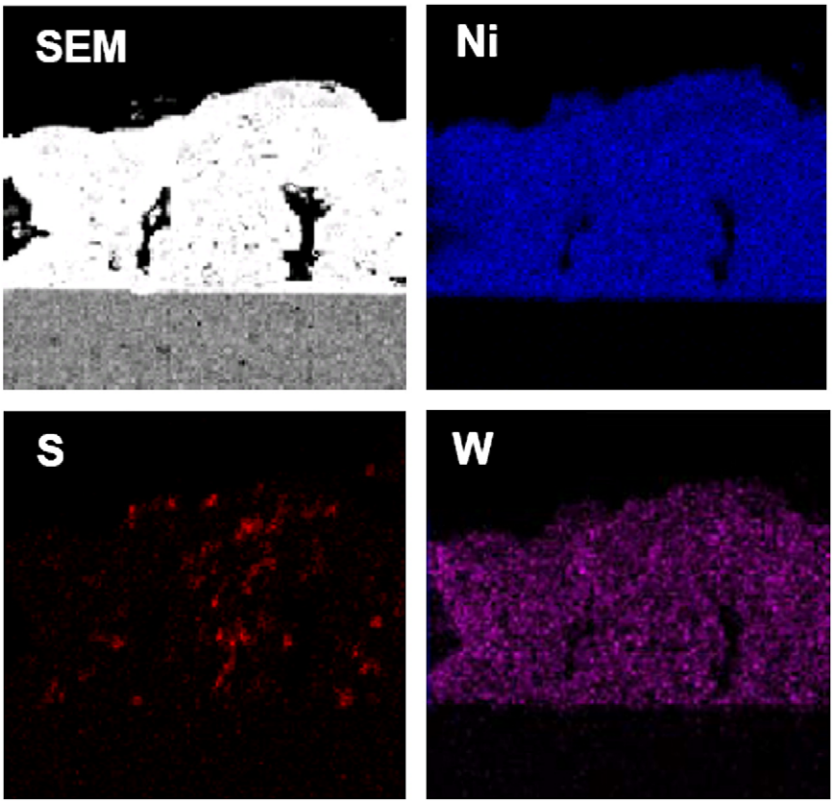

Fig. 4. SEM and EDS elemental mapping of cross section of Ni–W/MoS2 coating obtained with 0.5 g/L MoS_2 bath concentration. Ni, W and S maps are shown.

Fig. 3 shows cross section (left images) and top (right images) SEM images with the same magnification of Ni–W–MoS_2 composite coatings as a function of increasing MoS_2 bath concentration (A = 0 g/L, B = 0.5 g/L, C = 1 g/L, and D = 2 g/L). It is clear that the presence of the solid lubricant particles results in changes in the coating surface morphology and thickness. Coatings incorporating large concentration of MoS_2 particles (C and D) have higher surface roughness, higher thickness and an irregular sponge-like structure with large pores. Note that composite average thicknesses were measured directly in sample cross section images. The coating without MoS_2 (A) had a uniform thickness of ~40 μm, whereas coatings with MoS_2 had irregular morphologies with larger average thickness (B ~ 80 μm, C ~ 180 μm, and D ~ 250 μm). Therefore, composite coating thickness increases continuously as MoS_2 is increasingly incorporated into the coating. This is due to the formation of a sponge-like structure with large pores in the MoS_2 containing coatings.

Fig. 4 shows SEM and EDS elemental mapping images of the cross section of a Ni–W/MoS_2 coating obtained with 0.5 g/L of MoS_2 in solution. Ni Lα, W Mα, and S Kα lines were followed as a function of the coating cross section position. The S map shows that despite the coating irregular morphology there is no MoS_2 particle agglomeration within the coating. This is due to the fact that MoS_2 particles are dispersed in solution using a surfactant which prevented agglomeration during electrodeposition. Furthermore Fig. 4 also indicates that the black areas seen in the cross section images (Fig. 3) are due to pores present inside the coating. A direct consequence of this observation is that Ni–W–MoS_2 coatings with a pronounce sponge-like structure (MoS_2 bath concentration >1 g/L) have a weak adherence to the underlying substrate (the coating can be removed by scratching with a finger nail) and a very low hardness as indicated by the measurements shown in Fig. 2B.

As shown above, MoS_2 solid lubricant particles can be incorporated into a Ni–W nanostructured coating and its concentration in the coating can be controlled via the MoS_2 bath concentration. The results discussed above also indicate that MoS_2 bath concentrations (>1 g/L) resulted in Ni–W–MoS_2 composite coatings with very low microhardness (95% decrease), poor substrate adhesion and a porous sponge-like structure. On the other hand, Ni–W coatings with low MoS_2 content (bath concentration 0.5 g/L) have a somewhat compact structure with much fewer pores, good substrate adhesion and microhardness values comparable to the

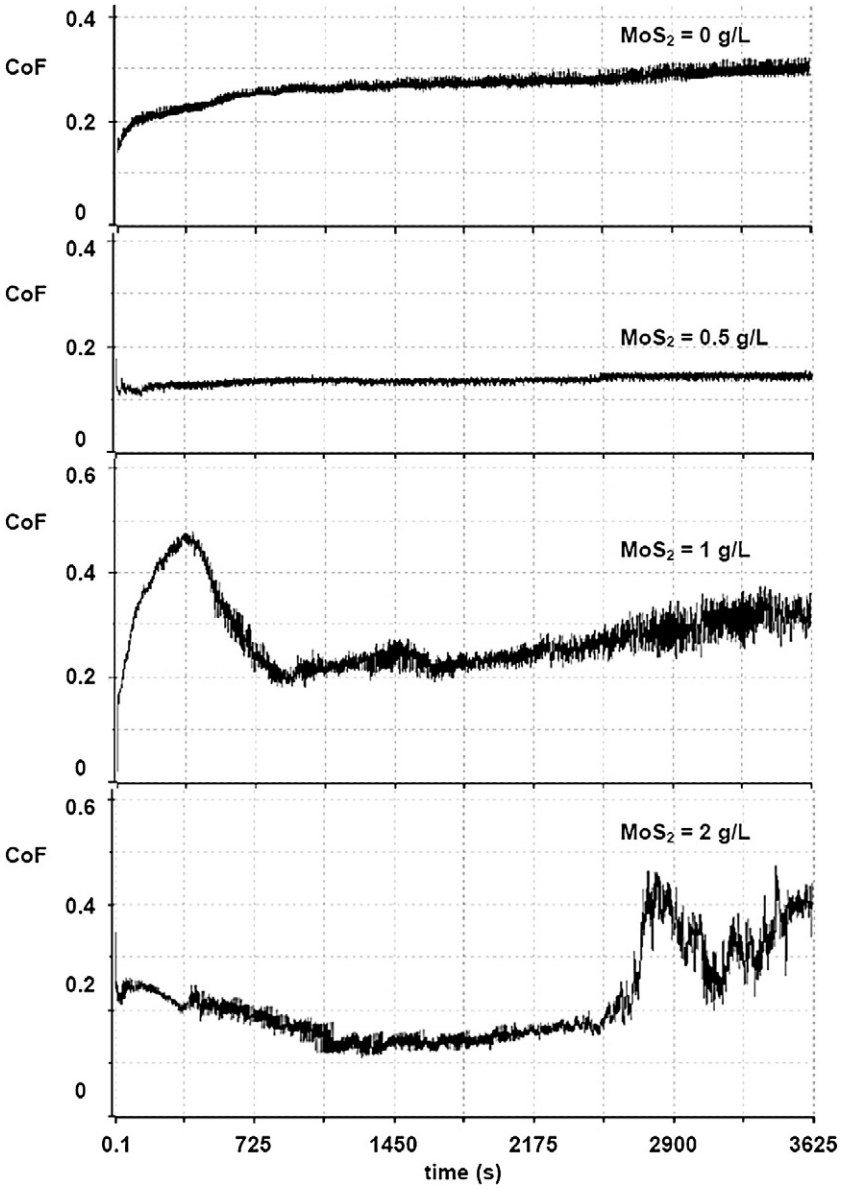

Fig. 5. Pin-on-disc measurements of the friction coefficient corresponding to Ni–W and Ni–W–MoS_2 nanostructured composite coatings.

unmodified coating (7% decrease). As we should discuss below these two different properties result in a very distinct frictional behavior.

Fig. 5 shows the friction coefficient (CoF) of Ni–W and Ni–W–MoS_2 coatings corresponding to 0, 0.5, 1 and 2 g/L MoS_2 bath concentration obtained via a pin-on-disc tribometer (coating thickness: ~40 μm, 80 μm, 180 μm and 250 μm respectively). Clearly, when Ni–W coatings have low MoS_2 content (bath concentration 0.5 g/L) CoF decreases from an average value of 0.27 to 0.14, i.e. incorporation of MoS_2 into the nanostructured Ni–W coating lowers the coating friction coefficient by ~50%. It should be noted that the measured CoF for Ni–W in the absence of the solid lubricant is in excellent agreement with CoF values reported in the literature (0.25) [23]. However, larger MoS_2 bath concentrations (1 g/L and 2 g/L) resulted in composite coatings with non constant friction coefficients with maximum values in excess of 0.4. As was mentioned above, these coatings present a sponge-like structure and very rough and inhomogeneous surfaces. This results in large deformation and wear and therefore friction curves are not smooth. Furthermore, these coatings easily detached from the substrate during the friction tests and therefore the high friction coefficient observed did not correspond to the coating itself but to the substrate and remains of the coatings. However, the important finding is that Ni–W–MoS_2 composite coatings with similar hardness and with friction coefficients ~50% lower than those corresponding to Ni–W coatings can be successfully electrodeposited employing low MoS_2 bath concentrations.

4. Conclusions

Ni–W–MoS_2 composite nanostructured coatings have been obtained by pulse plating techniques. Co-deposition of semiconducting molybdenum disulfide particles in the coating has an analog effect as decreasing the local current density during Ni–W electrodeposition: as the MoS_2 concentration in the coating increases both W content and coating microhardness decrease while the average grain size increases. Ni–W composite coatings have very dissimilar structural and frictional properties as a function of MoS_2 content. Large MoS_2 content (bath concentration >1 g/L) in Ni–W coatings results in rough surfaces, irregular sponge-like morphology, poor substrate adherence and irregular frictional curves. However, Ni–W composite coatings with low MoS_2 content (bath concentration ~0.5 g/L MoS_2) have lower friction coefficients and similar microhardness. Therefore, there is a solid lubricant concentration regime where co-deposition of MoS_2 particles into Ni–W nanostructured alloys enhances the frictional properties of the coating with a consistently lower friction coefficient.

Acknowledgements

The authors would like to thank Professor Christopher Schuh for useful discussions. Financial support from Tenaris is gratefully acknowledged. FJW is a fellow of the Argentinean National Research Council (CONICET). The authors would like to thank Romina Muñoz for her technical assistance during sample preparations.

References

[1] G.N.K. Ramesh Bapu, Plating Surf. Finish. (July 1995) 70.
[2] M. Pushpavanam, S.R. Natarajan, Met. Finish. (June 1995) 97.
[3] Y.C. Chang, Y.Y. Chang, C.I. Lin, Electrochim. Acta 43 (1998) 315.
[4] P. Berçot, E. Pena-Munoz, J. Pagetti, Surf. Coat. Technol. 157 (2002) 282.
[5] B. Szeptycka, A. Gajewska-Midzialek, Rev. Adv. Mater. Sci. 14 (2007) 135.
[6] M. Surender, B. Basu, R. Balasubramaniam, Tribol. Int. 37 (2004) 743.
[7] H.K. Lee, H.Y. Lee, J.M. Jeon, Surf. Coat. Technol. 201 (2007) 4711.
[8] M.R. Vaezi, S.K. Sadrnezhaad, L. Nikzad, Colloids Surf., A: Physicochem. Eng. Asp. 315 (2008) 176.
[9] L. Burzyńska, E. Rudnik, J. Koza, L. Błaż, W. Szymański, Surf. Coat. Technol. 202 (2008) 2545.
[10] T. Yamasaki, P. Schloβmacher, K. Ehrlich, Y. Ogino, Nanostruct. Mater. 10 (3) (1998) 375.
[11] C.A. Schuh, T.G. Nieh, H. Iwasaki, Acta Mater. 51 (2003) 431.
[12] A.J. Detor, C.A. Schuh, Acta Mater. 55 (2007) 371 and A.J. Detor, C.A. Schuh, Acta Mater. 55 (2007) 4221.
[13] N. Eliaz, T.M. Sridhar, E. Gileadi, Electrochim. Acta 50 (2005) 2893.
[14] M.D. Obradovic, G.Z. Bosnjakov, R.M. Stevanovic, M.D. Maksimovic, A.R. Despic, Surf. Coat. Technol. 200 (2006) 4201.
[15] K.R. Sriraman, S.G.S. Raman, S.K. Seshadri, Materials Science and Engineering A 418 (2006) 303–311 and Materials Science and Engineering A 460–461 (2007) 39.
[16] Y. Yao, S. Yao, L. Zhang, H. Wang, Mater. Lett. 61 (2007) 67.
[17] Y.W. Yao, S.W. Yao, L. Zhang, Mater. Sci. Technol. 24 (2) (2008) 237.
[18] G.V. Subba Rao, M.W. Schafer, in: F. Levy (Ed.), Intercalated Layered Materials, Reidel, Dordrecht, 1979, p. 99.
[19] Z. Zhang, F. Zhou, E.J. Lavernia, Metall. Mater. Trans. A 34A (2003) 1349.
[20] H. Iwasaki, K. Higash, T.G. Nieh, Scr. Mater. 50 (2004) 395.
[21] A. Giga, Y. Kimoto, Y. Takigawa, K. Higashi, Scr. Mater. 55 (2006) 143.
[22] T. Yamasaki, Mater. Phys. Mech. 1 (2000) 127.
[23] C.A. Schuh, T.G. Nieh, T. Yamasaki, Scr. Mater. 46 (2002) 735.